Available online at www.sciencedirect.com
ScienceDirect
Ceramics International 37 (2011) 1587–1591
CERAMICS INTERNATIONAL
www.elsevier.com/locate/ceramint

Dielectric and ferroelectric properties of $Ba_{0.8}Sr_{0.2}Ti_{1-5x/4}Nb_xO_3$ ceramics

Wan Q. Cao [a], Li Yang [a], Mukhlis M. Ismail [b,*], Ping Feng [a]

[a] Ministry-of-Education Key Laboratory for the Green Preparation and Application of Functional Materials, School of Material Science and Engineering, Hubei University, Wuhan 430062, China
[b] School of Applied Sciences, University of Technology, Baghdad, Iraq

Received 26 May 2010; received in revised form 10 November 2010; accepted 18 January 2011
Available online 18 February 2011

Abstract

$Ba_{0.8}Sr_{0.2}Ti_{1-5x/4}Nb_xO_3$ ceramics, $x = 0, 0.01, 0.05, 0.10$, were fabricated by conventional solid-state reaction. With increasing niobium content the ferroelectric phase transition temperature decreases linearly, and the dispersivity of the transition increases. Niobium B-site decreases transition temperature more pronounced than Sr^{2+} at A-site. The heterovalent substitution of Nb^{5+} in low content causes local defect dipole, while more substitutions introduce disorder to disturb the long-range dipole correlation. $Ba_{0.8}Sr_{0.2}Ti_{1-0.5/4}Nb_{0.1}O_3$ ceramic shows weak ferroelectric loop at room temperature far from its transition temperature, 153 K.

Keywords: $Ba_{0.8}Sr_{0.2}TiO_3$; Niobium; Relaxor ferroelectrics

1. Introduction

Barium strontium titanate ceramics ($Ba_{1-x}Sr_xTiO_3$ or briefly BST) are well known ferroelectric materials which have been used extensively as capacitor dielectrics for the last decades. Barium strontium niobate ($Ba_{1-x}Sr_xNbO_3$ or briefly BSN) ceramics have excellent ferroelectric [1,2] and pyroelectric properties [3–5]. BST has a high dielectric constant, good stability and mechanical properties [6], and BSN has attractive electro-optic properties [7,8]. BST is often employed to lower the Curie point for microwave devices, such as phase shifters, tunable filters, delay lines, and tunable oscillators [9,10]. The microstructure and properties of BST ceramics can be improved with heterovalent dopants [11].

Normal ferroelectrics have first-order phase transition at the Curie point (T_c) accompanied by a sharp permittivity peak, while relaxor ferroelectrics (relaxors) are characterized by a broad and frequency dependent maximum peak of permittivity. Relaxors are normally formed by doping foreign ions into the crystal lattice of ferroelectrics. There is an intermediate state between them, which is called the diffuse phase transition (DPT).

The dielectric properties of $Ba_{0.8}Sr_{0.2}TiO_3$ thin films have also been investigated [12], but the investigation of Nb_2O_5 doped $Ba_{0.8}Sr_{0.2}TiO_3$ has not been reported systematically. The transition temperatures of $Ba_{0.7}Sr_{0.3}TiO_3$ ceramics will decrease from room temperature by doping. The transition temperatures of $Ba_{0.8}Sr_{0.2}TiO_3$ ceramics can be controlled to room temperature by doping to obtain proper temperature dependent dielectric constant.

In this study, dielectric and ferroelectric properties of BST/BSN composite ceramics ($Ba_{0.8}Sr_{0.2}Ti_{1-5x/4}Nb_xO_3$) system were investigated. The characteristics of relaxors are discussed.

2. Experimental details

$Ba_{0.8}Sr_{0.2}Ti_{1-5x/4}Nb_xO_3$ (BSTN) ceramics with $x = 0$, 0.01, 0.05, 0.10 and $Ba_{1-y}Sr_yTiO_3$ (BST) ceramics with y ranging from 0 to 0.9 in 0.1 step, were prepared by the conventional mixed-oxide method with the starting materials of $BaCO_3$, $SrCO_3$, TiO_2 and Nb_2O_5 powders, which are shown in Table 1. The raw material was weighed out in stoichiometric proportions, ball-milled in alcohol, dried and then calcined at 1100 °C for 2 h. The obtained powders were pressed into pellets with a diameter of 11.8 mm and thickness of 1.0 mm prior to sintering at 1280 °C for 4 h. The silver paste was painted on the polished samples as the electrodes and fired at 800 °C for 10 min. The dielectric constant and loss of the samples were measured at

* Corresponding author.
E-mail address: mmismail009@gmail.com (M.M. Ismail).

0272-8842/$36.00
doi:10.1016/j.ceramint.2011.01.031

Table 1
Lattice constants and volume of $Ba_{0.8}Sr_{0.2}Ti_{1-5x/4}Nb_xO_3$ ceramics.

x	Composition purity	$BaCO_3$ (g) 99.0%	$SrCO_3$ (g) 99.0%	TiO_2 (g) 99.0%	Nb_2O_5 (g) 99.5%
0	$Ba_{0.8}Sr_{0.2}TiO_3$	11.9598	8.9472	4.8424	0
0.01	$Ba_{0.8}Sr_{0.2}Ti_{0.9875}Nb_{0.01}O_3$	11.9598	8.9472	4.7819	0.1603
0.05	$Ba_{0.8}Sr_{0.2}Ti_{0.9375}Nb_{0.05}O_3$	11.9598	8.9472	4.5398	0.8015
0.10	$Ba_{0.8}Sr_{0.2}Ti_{0.875}Nb_{0.10}O_3$	11.9598	8.9472	4.2371	1.6030

different temperatures and different frequencies by a HP 4192A LF Impedance Analyzer.

X-ray diffraction (XRD) with CuKα radiation (λ = 0.15406 nm) was performed to examine the phase structure of the specimens at room temperature. The ferroelectric hysteresis loops of ceramics were measured at room temperature by Radiant Precision Workstation (RT6000HVS, Radiant Technology, Inc.).

3. Results and discussion

Fig. 1 shows the X-ray diffraction patterns of the BSTN ceramic samples with different niobium contents. By comparing with a standard $Ba_{0.77}Sr_{0.23}TiO_3$ (JCPDS No. 44-0093, a = 3.977 Å, c = 3.988 Å), the XRD patterns confirm that the samples show only the pure phase without the tungsten bronze phase of BSN for four compositions sintered at 1280 °C for 4 h. Therefore, Nb^{5+} can occupy the site of Ti^{4+} in the crystal lattice without giving rise to a change of $Ba_{0.8}Sr_{0.2}TiO_3$ structure. However, a slight peak shift and peak broadening with increasing Nb content can be observed.

Fig. 2 shows the temperature dependence of dielectric constant (ε) with x = 0 (BST) at 1, 10 and 100 kHz. The ferroelectric to paraelectric phase transition temperature (T_c) is 68 °C (ε peak maximum). The phase transition peak is very sharp, which is in agreement with the results of Wu [13] and Kongtaweelert [14].

For pure $BaTiO_3$ ceramics, there are four structures and three transition temperatures as mentioned below:

$$\text{rhombohedral (R)} \xrightarrow{-80\,^\circ\text{C}} \text{orthorhombic (O)} \xrightarrow{5\,^\circ\text{C}} \text{tetragonal (T)} \xrightarrow{120\,^\circ\text{C}} \text{cubic (C)}$$

García [15] studied Nb_2O_5 doped $Ba_{0.7}Sr_{0.3}TiO_3$ materials and obtained four phases and three phase transitions at: $(R) \xrightarrow{\approx -110\,^\circ\text{C}} (O) \xrightarrow{\approx -50\,^\circ\text{C}} (T) \xrightarrow{\cong 30\,^\circ\text{C}} (C)$

The structure of $Ba_{0.8}Sr_{0.2}TiO_3$ has tetragonal phase at room temperature. There are three phase transitions in Fig. 2. The first transition occurs at 68 °C which belongs to a C/T transition of the material. This is in agreement with the findings in Ref. [16]. The peaks at −20 °C and −75 °C were T/O and O/R phase transition, respectively. Hence, the transition regulation is

$$(R) \xrightarrow{-75\,^\circ\text{C}} (O) \xrightarrow{-20\,^\circ\text{C}} (T) \xrightarrow{68\,^\circ\text{C}} (C)$$

Fig. 3 shows that the Curie point (C/T transition) decreases with Ba/Sr in $Ba_ySr_{1-y}TiO_3$ ceramics as

$$T_c = 23.04 + 519.76y - 152.43y^2, \quad (1)$$

with y denoting the Ba-content.

The dielectric measurement for x = 0.01, 0.05 and 0.10 was carried out. Fig. 4 shows that the widths of peaks of permittivity enlarge, and the DPT effect of the peaks of dielectric constant curves enhances with increase of Nb content.

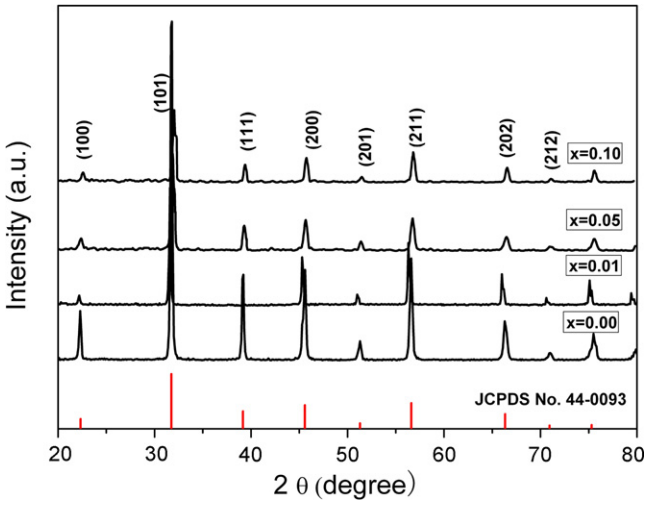

Fig. 1. XRD pattern of $Ba_{0.8}Sr_{0.2}Ti_{1-5x/4}Nb_xO_3$ ceramics sintered at 1280 °C for 4 h with Nb composition of x = 0, 0.01, 0.05, 0.10 measured at room temperature.

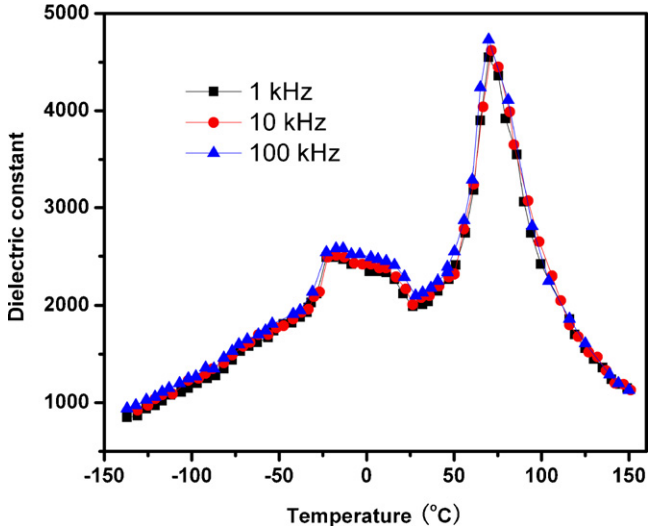

Fig. 2. Temperature dependence of dielectric constant for $Ba_{0.8}Sr_{0.2}TiO_3$ ceramics sintered at 1280 °C for 4 h.

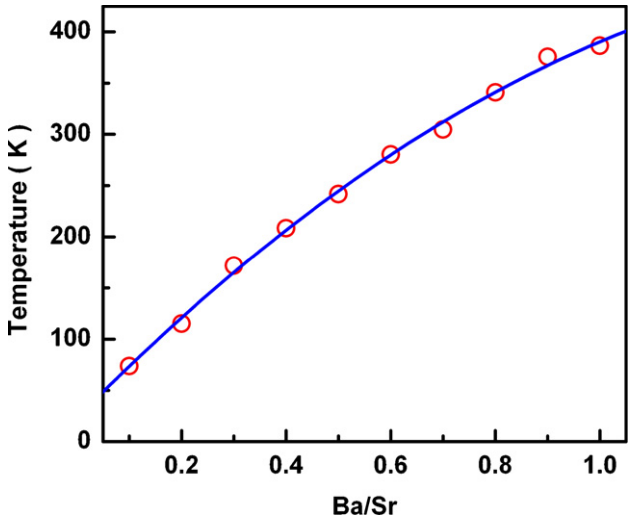

Fig. 3. Curie temperature versus Ba/Sr for $Ba_ySr_{1-y}TiO_3$ ceramics.

Fig. 5 exhibits that amount of Nb can reduce the phase transition temperature linearly. The fitting equation was obtained as

$$T_c\,(\mathrm{K}) = -1874.2x + 341, \tag{2}$$

with y denoting the Nb content.

The R/O phase transition was not analyzed, because the measurement was not very exact as the T/C phase transition in the present work and even in Ref. [15].

Compared with SrO doped $BaTiO_3$ at A-site, Nb_2O_5 is much more effective on decreasing transition temperature at B-site from Fig. 5 or Eq. (2).

The variation of inverse dielectric constant with respect to temperature is shown in Fig. 6. The dielectric behavior follows the modified Curie–Weiss law above the Curie point (T_c) in the form as [16]:

$$\log\left(\frac{1}{\varepsilon'} - \frac{1}{\varepsilon'_m}\right) = \log C + \gamma \log(T - T_m) \tag{3}$$

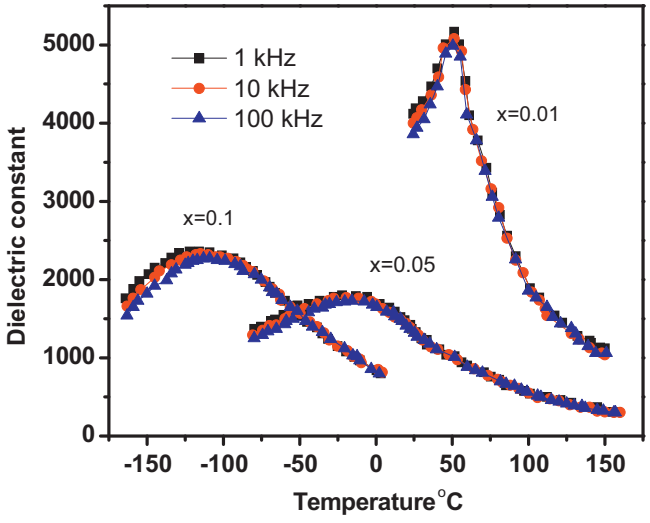

Fig. 4. Temperature dependence of dielectric constant for $Ba_{0.8}Sr_{0.2}Ti_{1-5x/4}Nb_xO_3$ ceramics sintered at 1280 °C for 4 h for $x = 0.01$, 0.05, and 0.10.

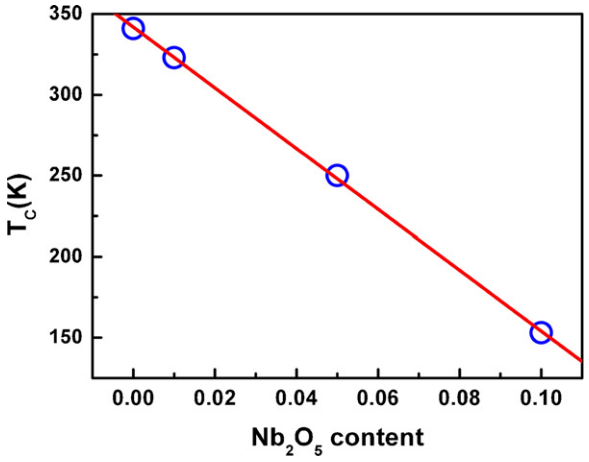

Fig. 5. Effect of niobium content on transition temperature for $Ba_{0.8}Sr_{0.2}Ti_{1-5x/4}Nb_xO_3$ ceramics from the results of Figs. 2 and 4 at 1 kHz frequency.

where ε_m and T_m represent the maximum of electric permittivity and the corresponding temperature, γ and C are fitting parameters to the experiment data. Fig. 7 shows the relationship between $\log((1/\varepsilon_r) - (1/\varepsilon_m))$ and $\log(T - T_m)$, and the straight lines are the fitting results by Eq. (3). The relation between γ and x can be fitted as the following equation:

$$\gamma = \frac{2.09}{1 + \exp[-33.7(x - 0.0115)]} \tag{4}$$

Fig. 8 shows a fit of γ with x from Fig. 7 by Eq. (4). The γ is 1.25 for $Ba_{0.8}Sr_{0.2}TiO_3$, which is close to the normal ferroelectric transition ($\gamma = 1$). The γ increases and DPT phenomenon enhances with the increase of Nb^{5+} content. Therefore, niobium substitution at B-site results in relaxor from ferroelectrics for $Ba_{0.8}Sr_{0.2}TiO_3$.

Fig. 9 shows electric hysteresis loops of $Ba_{0.8}Sr_{0.2}Ti_{(1-5x/4)}Nb_xO_3$ ceramics with $x = 0.05$ and 0.10 at room temperature. Remanent polarization, P_r, of $Ba_{0.8}Sr_{0.2}Ti_{(1-5x/4)}Nb_xO_3$ ceramics decreases with x. It is astonishing that the electric

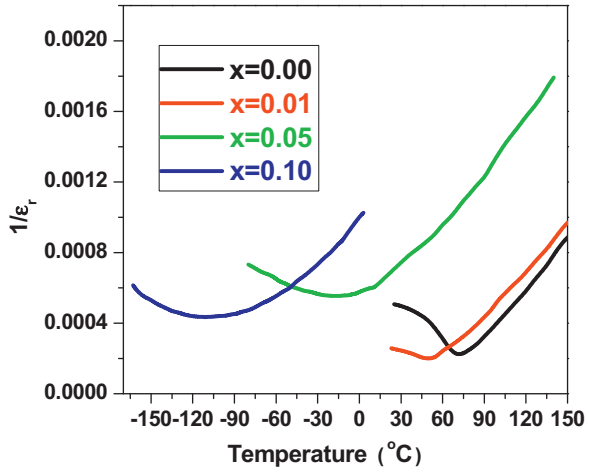

Fig. 6. Temperature dependence of the inverse dielectric constant for BSTN ceramics.

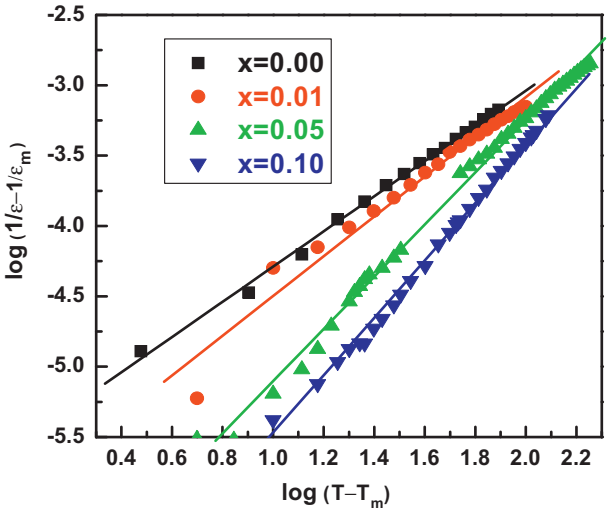

Fig. 7. Relationship between $\log(1/\varepsilon - 1/\varepsilon_m)$ and $\log(T - T_m)$ for BSTN. Solid lines are linear fits to experiment data.

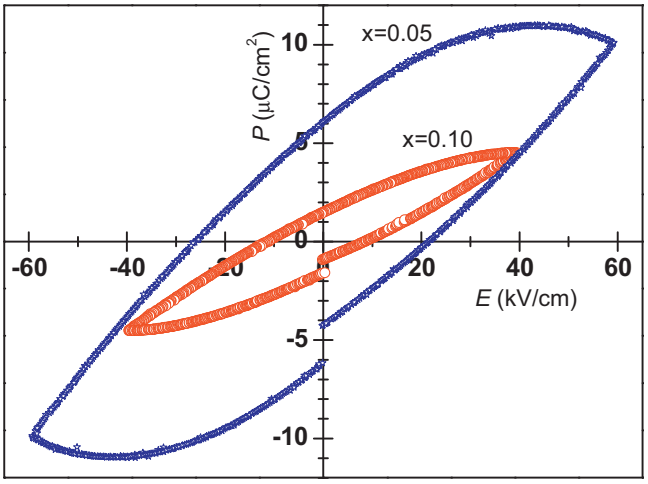

Fig. 9. Hysteresis loops of $Ba_{0.8}Sr_{0.2}Ti_{(1-5x/4)}Nb_xO_3$ for $x = 0.01, 0.05, 0.10$ at room temperature.

hysteresis loop can be detected for BSTN ceramic with $x = 0.10$, because the temperature difference is about 150 K from transition temperature to room temperature. The hysteresis loop of $Ba_{0.8}Sr_{0.2}Ti_{(1-5x/4)}Nb_xO_3$ ceramics with $x = 0.05$ bends on the top and bottom sides, which might be due to leakage currents. There is not any hysteresis loop when $x > 0.10$ due to formation of V_{Sr} and V_{Ti} and small amounts of second phase.

The effects of reducing phase transition temperature by adding SrO and Nb_2O_5 to $Ba_{0.8}Sr_{0.2}TiO_3$ are different. Hysteresis loop is changed to a line for $Ba_{0.6}Sr_{0.4}TiO_3$ ceramics at room temperature with Curie temperature near 280 K [16], while a hysteresis loop still exists for $Ba_{0.8}Sr_{0.2}Ti_{(1-0.5/4)}Nb_{0.1}O_3$ ceramics at room temperature with a relaxor ferroelectric transition at 153 K. This result indicates that the effects of niobium substitution for titanium on dielectric and ferroelectric properties are different from those caused by Sr substitution on the Ba site. Dielectric constant peak drops to low temperature rapidly, but ferroelectricity weakens slowly. Imperfection disturbing the dipole correlation is the possible reason.

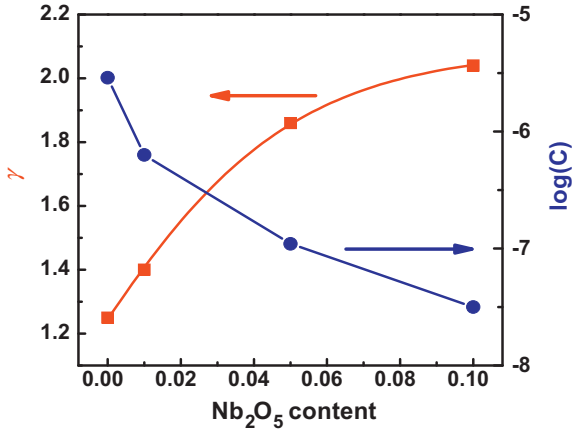

Fig. 8. Variation of γ and $\log C$ versus x for $Ba_{0.8}Sr_{0.2}Ti_{1-5x/4}Nb_xO_3$. Solid square represents γ, and corresponding line is a fit by Eq. (4). Solid circle represents $\log C$.

4. Conclusion

The dielectric and relaxor ferroelectric characteristics of niobium doped barium strontium titanate ceramics have been investigated. The XRD patterns exhibit that Nb^{5+} can occupy the site of Ti^{4+} in the crystal lattice. The phase transition temperature shifted to lower temperature is a linear relationship with Nb_2O_5 content. The relaxor property of ferroelectric phase transition is enhanced by niobium dopant. The action mechanisms of Nb^{5+} on dielectric property for BST can be inferred that heterovalent substitution at B-site causes lattice imperfections to produce local defect dipoles and due to electronic compensation for niobium content less than 0.05, and disturbs long-range dipole correlation to decrease phase transition temperature to 153 K for 0.10 niobium content, but ferroelectricity remains to room temperature.

Acknowledgement

Authors thank the support from the Research Foundation of Science and Technology Bureau of Hubei Province, China (Grant No. D 2009CDB027).

References

[1] G.W. Dietz, M. Schumacher, R. Waser, S.K. Streiffer, C. Basceri, A.J. Kingon, Leakage currents in $Ba_{0.7}Sr_{0.3}TiO_3$ thin films for ultrahigh-density dynamic random access memories, J. Appl. Phys. 82 (1997) 2359–2364.

[2] J.G. Cheng, J. Tang, J.H. Chu, A.J. Zhang, Pyroeletric properties in sol–gel derived barium strontium titanate thin films using a highly diluted precursor solution, Appl. Phys. Lett. 77 (2001) 1035–1037.

[3] R.W. Whatmore, R. Watton, Pymelectric ceramics and thin films for uncooled thermal imaging, Ferroelectrics 236 (2000) 259–279.
[4] R. Owen, J. Belcher, H. Beratan, in: E.L. Dereniak, R.E. Sampson (Eds.),Infrared detectors and focal plane arrays IV, SPIE (Orlando) 2746 (1996) 101–112.
[5] C. Duran, M.T. Susan, L.G. Messing, Fabrication and electrical properties of textured $Sr_{(0.53)}Ba_{(0.47)}Nb_2O_6$ ceramics by templated grain growth, J. Am. Ceram. Soc. 83 (2000) 2203–2212.
[6] S.K. Tae, H.K. Chang, H.O. Myung, The effect of buffer layer on the structural and electrical properties of (BaSr)Ti0_3 thin films deposited on Indium tin oxide-coated glass substrate by using a rf magnetron sputtering method, J. Appl. Phys. 7 (1994) 4316–4322.
[7] T. Granzow, Th. Woike, W. Rammensee, Influence of Ce and Cr doping on the pyroelectric behaviour of $Sr_{0.61}Ba_{0.39}Nb_2O_6$, Phys. Stat. Sol. A 197 (2003) R2–R4.
[8] Y.L. Zhang, D. Mo, E.Y.B. Pun, L.P. Shi, X.S. Xie, Growth and photorefractive properties of Mn-doped $(KNa)_{(0.1)}(Sr_{0.6}Ba_{0.4})_{(0.9)}Nb_2O_6$ crystals, J. Appl. Phys. 79 (1996) 8835–8837.
[9] H.V. Alexandru, C. Berbecaru, A. Ioachim, M.I. Toacsen, M.G. Banciu, L. Nedelcu, D. Ghetu, Oxides ferroelectric (Ba, Sr)TiO_3 for microwave devices, Mater. Sci. Eng. B 109 (2004) 152–159.
[10] E.A. Parker, S.B. Savia, B active frequency selective surfaces with ferroelectric substrates, IEE Proc. Microw. Antennas Propag. 148 (2) (2001) 103.
[11] X.Y. Wei, X. Yao, Nonlinear dielectric properties of barium strontium titanate ceramics, Mater. Sci. Eng. B 99 (2003) 74–78.
[12] G.C. Jha, S.K. Ray, I. Manna, Effect of deposition temperature on the microstructure and electrical properties of $Ba_{0.8}Sr_{0.2}TiO_3$ thin films deposited by radio-frequency magnetron sputtering, Thin Solid Films 516 (2008) 3416–3421.
[13] R. Wu, P.Y. Du, W.J. Wen, G.R. Han, Preparations and dielectric properties of $Ba_{0.80}Sr_{0.20}TiO_3$/PbO–B_2O_3 thick films, Mater. Chem. Phys. 97 (2006) 151–155.
[14] S. Kongtaweelert, D.C. Sinclair, S. Panichphant, Phase and morphology investigation of $Ba_xSr_{1-x}TiO_3$ (x = 0. 6, 0. 7 and 0. 8) powders, Curr. Appl. Phys. 6 (2006) 474–477.
[15] S. García, R. Font, J. Portelles, R.J. Quiñones, J. Heiras, J.M. Siqueiros, Effect of Nb doping on (Sr,Ba)TiO_3 (BST) ceramic samples, J. Electroceram. 6 (2001) 101.
[16] C.L. Fu, C.R. Yang, H.W. Chen, Y.Z. Wang, L.Y. Hu, Microstructure and dielectric properties of $Ba_xSr_{1-x}TiO_3$ ceramics, Mater. Sci. Eng. B 119 (2005) 185–188.